CB01 - Effect of Mechanical Stress on Pitch Distribution during Anode Baking

Nafiseh Shadvar[1], Guillaume Gauvin[2], Simon Laliberté-Riverin[3], Julien Lauzon-Gauthier[4] and Houshang Alamdari[5]

1. PhD Candidate
2. Research Professional
3. Postdoctoral Fellow
5. Full Professor

Department of Mining, Metallurgical, and Materials Engineering, Université Laval, Québec, Canada

Aluminium Research Centre - REGAL, Université Laval, Québec, Canada

4. Research Engineer

Alcoa Corporation, Continuous Improvement Smelting Technology, Québec, Canada

Corresponding author: nafiseh.shadvar.1@ulaval.ca

Abstract

The baking process is a critical step in carbon anode production, during which significant microstructural evolutions take place in anodes. Anode sticking is one of the industrial challenges affecting anodes after baking. It refers to either anodes sticking together or packing coke adhering to the anode surface, resulting in increased anode losses and overall production costs. Since many anodes are vertically stacked together in the baking furnace, the mechanical stress generated by the weight of the top anodes may lead to viscous pitch squeezing out of the bottom anodes during baking, which is thought to enhance anode sticking. This work aimed to investigate the presence of pitch squeezing out of anodes by studying the influence of uniaxial compressive stress on pitch distribution. A marker was added to the pitch so that the pitch distribution could be monitored by elemental mapping using XRF spectrometry. Pitch marker development was performed by choosing three oxides (ZnO, FeO, Bi_2O_3) and using different mixing procedures. Lab-scale anodes were then fabricated with an optimized pitch ratio having 1 wt.% Bi_2O_3 as a chosen marker. Green anodes were subsequently baked under uniaxial compressive stresses of 0 kPa, 25 kPa, and 50 kPa, corresponding to the stresses exerted on the top, middle, and bottom anodes in the industrial furnace, respectively. The results indicated that the mechanical stress impacted baked anode properties by decreasing electrical resistivity, although apparent density variation was not significant. XRF analysis revealed a considerable difference in Bi distribution between green and baked anodes. Significant pitch dispersion over baked anodes determined the pitch tendency to squeeze out of the anodes, which can be used to explain the anode sticking. Additionally, pitch marker application was revealed to be a suitable method to trace pitch distribution after baking to eventually correlate it with anode sticking issue.

Keywords: Carbon anode, Anode sticking, Packing coke, Pitch distribution, Mechanical stress.

1. Introduction

Carbon anode is an essential part of the primary aluminium production in the Hall-Héroult process as it conducts electrical current and acts as a reducing agent [1]. The anode is consumed during electrolysis and for producing one ton of Al, between 400 kg and 450 kg of the anode is consumed [2]. The anode is made by compacting and baking an anode paste. The anode paste is obtained by mixing two main constituents, i.e., calcined petroleum coke (CPC) as dry aggregate and coal-tar-pitch (CTP) as binder, to which recycled anode butts could also be added. The resultant anode paste is then compacted, forming a green anode which is subsequently baked at 1100 °C – 1200 °C. To prevent anode oxidation during baking in the furnace, packing coke is

poured between the anode and the furnace refractory walls [1, 3]. During the heating cycle in the furnace, solid pitch changes to liquid phase at about 120 °C – 220 °C, releases volatiles and transforms to coke at higher temperatures [3, 4]. The released volatiles escape from the anode and if the rate of volatile generation exceeds the rate of its escape through the porous structure of the anode, it may create an internal pressure in the anode during baking [4]. The baking process is a critical step contributing to the desired physical, mechanical, and electrical properties in the resulting anode block.

It is frequently observed that the packing coke sticks on the anode surface (Figure 1). In some cases, even two anodes, piled over each other in the furnace, may stick together. These phenomena are known as "anode sticking", which is an industrial challenge [5] since the stuck anodes require not only additional operator interventions for unloading the furnace after baking, but they also need serious safety considerations for being carried from the furnace to their next positions. Moreover, anode sticking leads to material loss due to discarding anodes in case of breakage or severe coke sticking [6, 7]. Stuck coke also fills anode slots, requiring anode slotting machines to regenerate them. Consequently, anode sticking results in a significant increase in overall production costs.

Figure 1. Sticking of packing coke to anode blocks (Courtesy of Alcoa Corporation).

Several investigations have been performed to identify the primary reasons leading to anode sticking. Most of them have revealed that overpitching greatly contributes to anode sticking owing to excessive released volatiles during baking [5, 6]. Besides, low Blaine Number of fine coke as well as low quantity of fineness at a constant pitch ratio have been demonstrated to cause anode sticking [5]. Meanwhile, anode sticking has also been attributed to compacting process conditions, including high forming pressure and severe vacuum usage [5, 8]. Despite these reported observations, no systematic study has been carried out to rationalize the effect of different parameters on anode sticking.

In industrial baking furnaces, three anodes are generally stacked on top of each other, generating mechanical stresses on the lower anodes [9]. Therefore, it is reasonable to hypothesize that liquid viscous pitch squeezes out of the anodes during baking, due to the stress induced by the weight of the top anodes and enhances the anode sticking phenomenon. The effect of this induced stress has also been reported on the electrical conductivity of the bottom anodes [9]. However, to the best of our knowledge, no study has examined the effect of the vertical position of the anodes (externally induced mechanical stress during baking) on the anode sticking. Therefore, the objective of this work was to determine the influence of uniaxial compressive stress on the flow of the pitch and to reveal if it is squeezed out of the anodes during baking. To reveal the pitch flow, the pitch distribution was tracked in the cross-section of the baked anode. Once the pitch squeezing is observed, it can be correlated with anode sticking in future studies. For the aim of this paper, an optimized pitch ratio was first determined for a certain type of coke and pitch. Then, a suitable pitch marker was used to be able to track pitch in the green and baked anodes. The pitch

marker was added to the pitch prior to mixing the anode paste constituents. Lab-scale anodes were then fabricated, and steel weights were used to bake the anodes with various uniaxial compressive stresses corresponding to different vertical positions in typical industrial furnaces. The anodes were finally characterized in terms of properties and marker distribution.

2. Materials and Methods

2.1 Raw Materials

Calcined petroleum coke (CPC) and coal tar pitch (CTP) were provided by Alcoa Corporation (Deschambault, Quebec, Canada). The chemical composition of CPC, obtained using a Rigaku ZSX Primus X-ray fluorescence (XRF) spectrometer (Rigaku Corporation Tokyo, Japan), is presented in Table 1. The physical properties and chemical composition of the CTP, which were provided by Alcoa Corporation, are also represented in Table 2. It should be emphasized that no recycled anode butts were used in lab-scale anodes.

Table 1. Chemical composition of CPC obtained in weight basis.

Element (ppm)	C (%)	S (%)	Na	Al	Si	Fe	V	Ca	Cl	Ni	Zn	P
Coke	98.0	1.73	853	502	393	442	300	177	138	180	21	20

Table 2. Physical properties and chemical composition of CTP.

Softening point (°C)	**Quinoline insoluble (%)**	**Coking value (%)**	**Ash (%)**	**Water (%)**	**Chemical Composition (ppm)**					
					S (%)	**Na**	**Si**	**Fe**	**Ca**	**Pb**
114	8.3	56	0.11	1.5	0.61	18	83	86	47	178

2.2 Laboratory-Scale Anode Preparation

To fabricate laboratory-scale anodes, calcined petroleum coke was first crushed, sieved, and classified into various size distributions, as depicted in Table 3. The dry aggregate recipe was selected based on the previous research [10]. The coke fractions were preheated at 178 °C for at least 15 h in a laboratory oven (GCA/Precision Scientific, Chicago, IL, USA). It was followed by adding the solid pitch to the coke, leaving the mix at the same temperature for 30 min and mixing subsequently for 10 min in a Hobart N50 mixer (Hobart, OH, USA). The resultant paste was compacted with a uniaxial compressive stress of 60 MPa at 150 °C using an MTS servo-hydraulic press (MTS Systems, Eden Prairie, MN, USA), to form a cylindrical green anode with dimensions of 50 mm diameter × 100 mm length. Finally, the cooled green anode was baked in a laboratory furnace (IFS 363635 Pyradia, Canada) at 1100 °C [10]. Figure 2 shows the temperature profile during the baking process, starting from room temperature to reach 150 °C in 2 h (60 °C/h), then to 650 °C in 25 h (20 °C/h), next to 1100 °C in 9 h (50 °C/h), and eventually switching off to cool down after 20 h soaking time.

Table 3. Petroleum coke size fractions and their percentages in dry aggregate [10].

Coke (US mesh)	-4 +8	-8 +14	-14 +30	-30 +50	-50 +100	-100 +200	Fine (BN 4500)
Wt. (%)	21.8	10.0	11.5	12.7	8.8	10.8	24.2

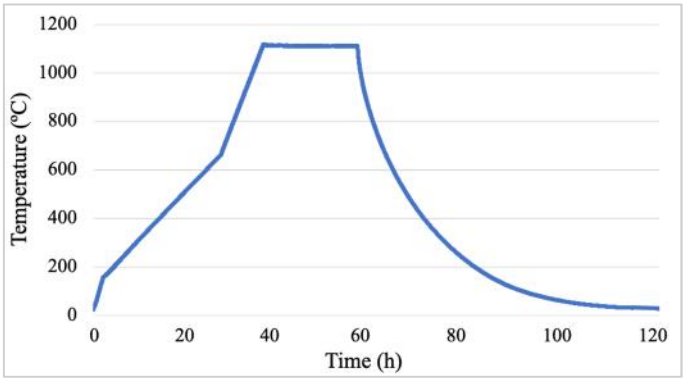

Figure 2. Temperature profile of laboratory baking furnace.

2.3 Pitch Optimization

Basically, optimum pitch demand (OPD) is required to be attained for a given coke aggregate, pitch binder, and fixed processing conditions. It corresponds to the amount of pitch content for which the baked anode density (BAD) is maximal [6, 11]. To determine the OPD, different pitch/coke ratios (P/C) in the range of 14/100 to 23/100, were used to produce lab-scale anodes. The P/C ratio refers to the mass ratio of pitch (g) per 100 g of coke, generally known as pitch ratio (%) [12]. Anode pastes were then prepared a constant mass of 312 g. Three anodes were produced for each pitch ratio to ensure the repeatability of the results. The green and baked apparent densities (GAD, BAD) of the anodes were then measured using the standard ASTM D5502-00 test method.

2.4 Pitch Marker Development

To trace the pitch distribution in the anode, a marker was first developed. Such a marker should have certain characteristics, i.e., it should not alter the rheological properties of the pitch, it should be traceable by the routine characterization techniques such as XRF or X-Ray tomography, it should be well dispersed in liquid pitch and, ideally, it should not react with pitch nor affect its polymerization reactions. Therefore, three metallic oxides in fine powder form elements (ZnO, FeO, and Bi_2O_3) were targeted to be mixed with CTP in low quantity of one weight percent (1 wt.%). Prior to mixing them with pitch, the powders were ball-milled using a high-energy ball mill (SPEX-8000® SamplePrep, USA.), and sieved to obtain particles smaller than 20 µm. The resultant powders were then mixed with either preheated or solid crushed pitch and were heated in an oven at 178 °C for 30 min. The pitch-oxide mixtures in liquid form were then blended using a mechanical stirrer for 10 min and poured subsequently on an aluminium plate to cool down. Table 4 represents mixing procedures carried out to attain an acceptable oxide distribution in pitch.

Table 4. Mixing procedures used to fabricated CTP-oxide samples.

Mixture	Mixing procedure			
	Ball-milling	Sieving	Adding oxide	Mechanical stirrer
CTP-ZnO	No	No	To preheated pitch	5 min
CTP-FeO	Yes	No	To preheated pitch	10 min
CTP-Bi_2O_3	Yes	Yes	To solid pitch	10 min

The solidified pitch-oxide samples were mounted in an acrylic-based resin (Buehler Ltd. IL, USA). The samples were then polished on silicon carbide papers at 240, 320, 400, 600, and 800 grits using LECO polishing table (LECO Corporation, St. Joseph. Michigan, USA.). It was followed by polishing on a PAN-W (LECO Corporation) cloth paper with 9 microns and 1 micron diamond suspensions. The final polishing was conducted on an Imperial cloth paper (LECO Corporation) with colloidal silica suspension (SiO_2) (OP-U NonDry, Struers ApS, Denmark). Afterward, the polished samples were prepared for the scanning electron microscopy (SEM) and energy dispersive spectroscopy (EDS) by application of a carbon coating with 25 nm thickness using an Edwards E306A Coating System. These SEM analyses were carried out using an SEM device (TESCAN Model Type: VEGA3) to determine the distribution of marker in the CTP. An acceleration voltage of 15 kV and a working distance of 15 mm were selected. In addition, the coking value (CV) of the pitch-oxide mixtures was measured based on the standard ISO 6998:1997 to examine the impact of adding 1 wt. % oxide on the pitch residue after carbonization. For better reliability, CV tests were repeated three times on each sample. The selected pitch marker corresponded to the oxide possessing better dispersion in the pitch without affecting its coking value.

2.5 Baking Marked Anodes under External Mechanical Stress

Lab-scale anodes were made with the marked pitch, using the optimum pitch content, as obtained previously. Some green anodes were baked with uniaxial compressive stress. According to the anode positions in the industrial furnaces shown in Figure 3-a, mechanical stresses of σ_1, σ_2, and σ_3 are exerted on the top, middle, and bottom anodes, respectively. Considering a 1000 kg industrial anode with 0.38 m^2 of cross-sectional area, the mechanical stresses are obtained by Equation (1), Equation (2), and Equation (3). It is noted that the weight of the packing coke is neglected [9].

$$\sigma_1 = 0 \tag{1}$$

$$\sigma_2 = \frac{m_{anode} \times g}{A} = 25 \text{ kP} \tag{2}$$

$$\sigma_3 = \frac{2 \times m_{anode} \times g}{A} = 50 \text{ kPa} \tag{3}$$

where:

σ_1, σ_2, σ_3	Mechanical stress, Pa
m_{anode}	Mass, kg
g	Gravitational constant, 9.8 m/s^2
A	Cross sectional surface area, m^2

To mimic the external compressive stress on the anode samples during baking, round bars of 1045 steel (density ρ = 7.87 g/cm^3) were used to apply equivalent uniaxial compressive stresses on the anodes. Based on the lab-scale anode diameter (50 mm), the steel bar mass was calculated as m_2 = 5 kg for σ_2 and m_3 = 10 kg for σ_3. The baking setup and steel bar dimensions are illustrated in Figure 3-b.

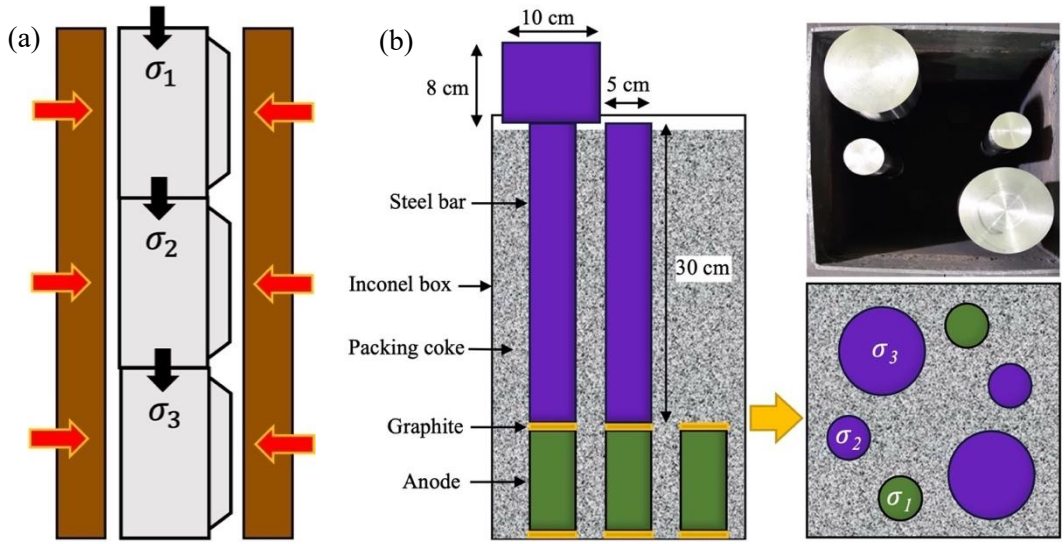

Figure 3. (a): Anode positions in baking furnaces, (b): Side view and top view of the samples in the furnace with steel bars.

2.6 Anode Characterization

The green and baked densities of the anodes were measured according to the ASTM D5502-00 standard test method. It was hypothesized that during baking with the uniaxial compressive stress, anodes are expanded in the central part of the length, similar to workpiece expansion in open die forging, a phenomenon known as the "Barreling effect" [13]. Therefore, the diameters of the baked anodes were measured on 9 sections throughout the sample length to not only determine the apparent density more precisely, but also to verify the existence of the barreling effect owing to the compressive stresses.

The specific electrical resistivity (SER) of the baked anodes was determined according to the ISO 11713 standard test method. The sample is fixed longitudinally between two steel plates using springs on both sides with a compressive stress of 3 MPa, as shown in Figure 4-a. A current of 1 A is applied through the sample using a DC power supply, and the voltage drop is measured on the surface of the specimen using a two-pin sensor [10, 14]. Moreover, the Van der Pauw (VDP) method was used to measure the SER of the samples after cutting them into small pieces of a thickness of 25 mm from the bottom section of the lab-scale anodes. This technique is considered to measure accurately the inherent electrical resistivity of the material since the influence of the sample surface defects is minimal. In the VDP method, the specimen is placed in a setup consisting of four V-shaped copper probes. A current of 1 A passes through two contiguous probes, and the voltage is measured between two other adjacent probes (Figure 4-b). The SER is calculated using Equation (4) [14, 15].

$$e^{-\pi.\frac{L}{\rho}R_{AB,DC}} + e^{-\pi.\frac{L}{\rho}R_{BC,AD}} = 1 \quad (4)$$

where:

L	Sample thickness, m
$R_{AB,DC}$	Electrical resistance (for the current of A and B, and the voltage of D and C), μΩ
$R_{BC,AD}$	Electrical resistance (for the current of B and C, and the voltage of A and D), μΩ
ρ	Electrical resistivity, μΩm

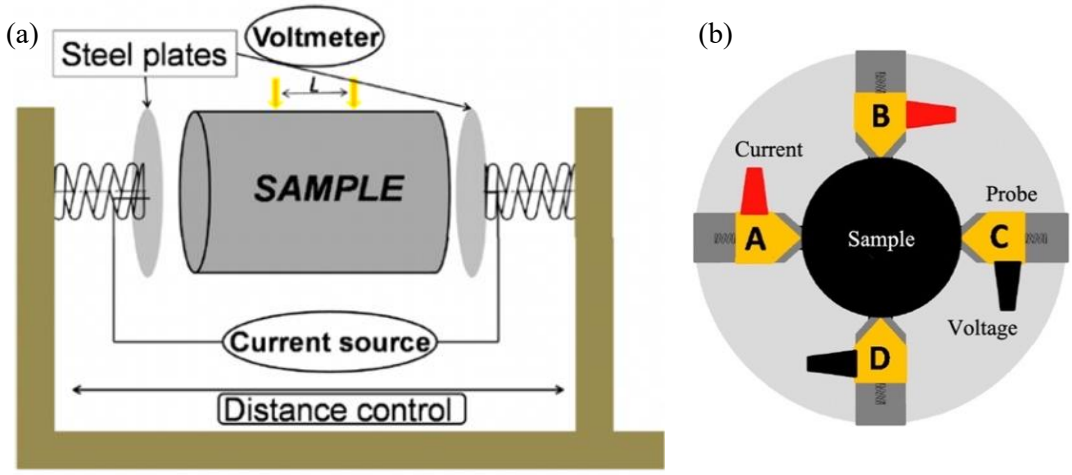

Figure 4. Schematic representation of (a): Standard two-point probe method and (b): VDP method for SER measurement [14].

Next, the small-scale specimens, sliced for SER measurement, were polished with silicon carbide papers at 120, 240, 320, 400, 600, and 800 grits using the LECO device to gain a smooth surface for further characterizations. The samples were then dried in an oven at about 40 °C for 48 h. X-ray fluorescence (XRF) elemental mapping of the polished green and baked samples was conducted using μ-XRF Tornado M4 (Bruker) at 50 kV to trace the pitch marker on the cross-section of the specimens. Furthermore, XRF elemental composition was carried out to determine the concentration of pitch marker in all specimens using a Rigaku ZSX Primus XRF spectrometer (Rigaku Corporation Tokyo, Japan). Due to the small effective radius of analysis (10 mm), it was not possible to map the whole sample surface. Thus, the analysis was performed on three circles with 10 mm diameter from the center toward the edge of the specimens to follow the variation of the element concentration. Finally, SEM and EDS analyses were performed to examine the probable evolution in the chemical structure of the oxide during anode baking. Anode characterizations were replicated on three samples for each set of preparation conditions to ensure the reliability of the results.

3. Results and Discussions

3.1 Pitch Optimization

Figure 5 shows the green and baked apparent densities as a function of pitch ratios. The GAD increases monotonically as the pitch content increases, since there is more pitch available to fill in the gaps of the coke particles and to penetrate inside coke pores, thus increasing the GAD. The baked anode density (BAD), however, reaches a peak and then starts decreasing. This is known behavior and is attributed to the fact that with a pitch content higher than the optimum value, excessive volatiles are released from the anode during baking, leaving the baked anode with more porosity and lower BAD [5]. Based on these results, the optimum pitch ratio was determined to be 18%, equivalent to a pitch percentage of 15.25 % in total green anode mass, which also represents optimum pitch demand (OPD). At this ratio, the BAD was determined to be 1.54 g/cm^3.

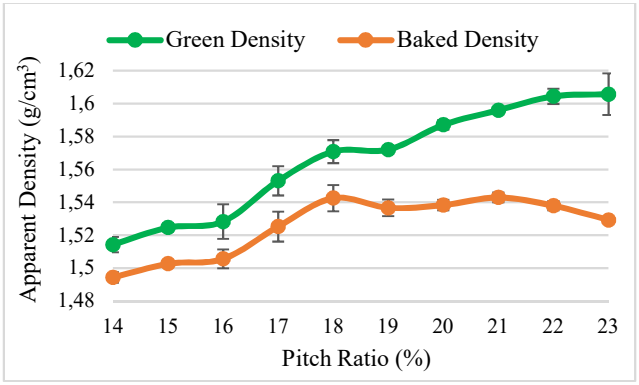

Figure 5. GAD and BAD for various pitch ratios. Error bars show the standard deviation.

3.2 Pitch Marker

Figures 6 (a, b) illustrate the SEM images in Backscattered Electron (BSE) mode for the CTP-ZnO and CTP-FeO samples respectively at 100X magnification. The bright spots represent the elements with higher atomic number, i.e., Zn and Fe. High degrees of agglomeration can be observed for the oxide particles inside the pitch. However, a relatively homogeneous distribution of Bi was detected even at 500X magnification (Figure 6-c). Additionally, the EDS spectra of Spot 1 represented in Figure 6-d verifies the presence of Bi as bismuth oxide in the sample. The atomic percentage ratio of Bi/O is approximately 2/3, implying that the chemical bond of Bi_2O_3 remained stable by mixing with the pitch at 178 °C. It signifies that the last mixing procedure worked well in achieving an appropriate distribution of Bi_2O_3 in the pitch. Besides, coking value (CV) was determined to be 58.3 % (± 0.4 %) for pure CTP and 59.0 % (± 0.7 %) for CTP-Bi_2O_3, showing an insignificant change in CTP carbonization by adding 1 wt. % Bi_2O_3.

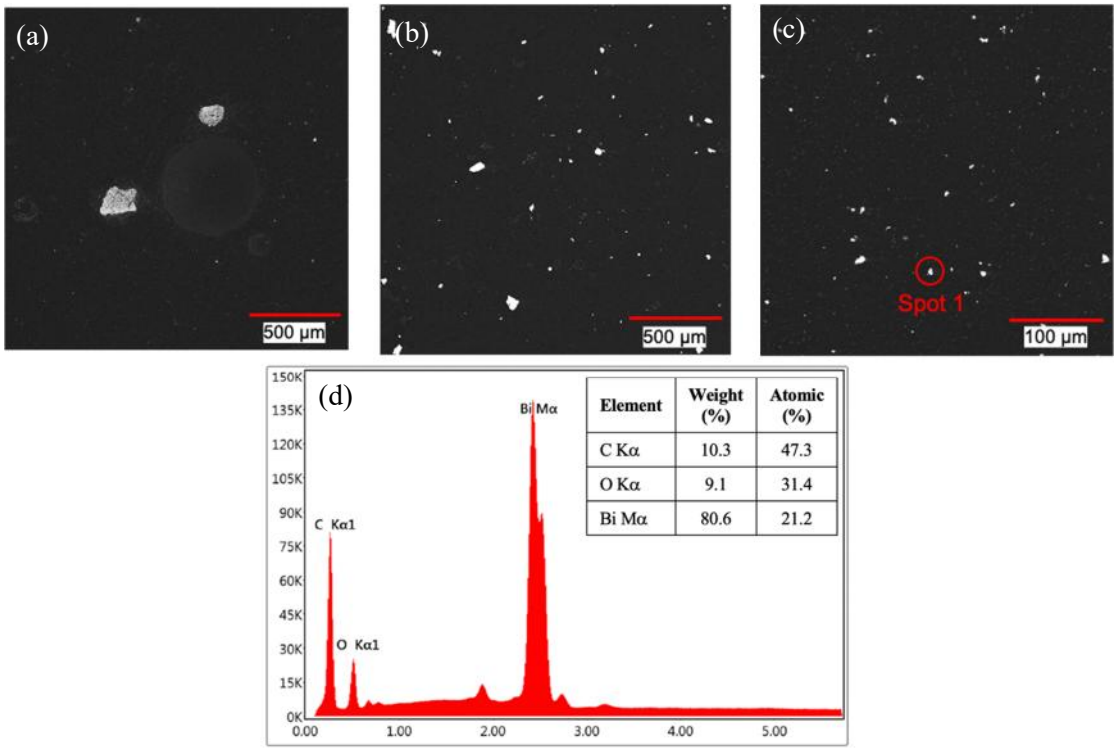

Figure 6. SEM images of (a): CTP-ZnO, (b): CTP-FeO, and (c): CTP-Bi_2O_3 in BSE mode, (d): EDS spectra of Spot 1.

Consequently, Bi was determined as the proper pitch marker to mix with the pitch in the form of Bi_2O_3 owing to two reasons. First, Zn and Fe were both primary contaminants in the petroleum coke (Table 1), while the anode required a unique traceable foreign element existing only in the pitch. Second, Bi has high atomic mass making it easily distinguished from other elements and it exhibits very low agglomeration in the pitch.

3.3 Anode Characterization

- **Apparent Density and Barreling Effect**

Figure 7-a represents GAD and BAD for the green anodes and the anodes baked under different compressive stresses. The green densities of all samples are in the same range, suggesting that there is no bias related to the initial green density variation. Although the mean baked densities increase by 0.5 % from 0 kPa to 50 kPa compressive stress, one-way analysis of variance (ANOVA) revealed that the difference in mean densities is not statistically significant (*p*-value was calculated 0.101). It implies that a slight increase in baked densities cannot be accurately attributed to closing more voids and reducing the space between coke particles due to high stress and more experiments need to be conducted to verify this hypothesis.

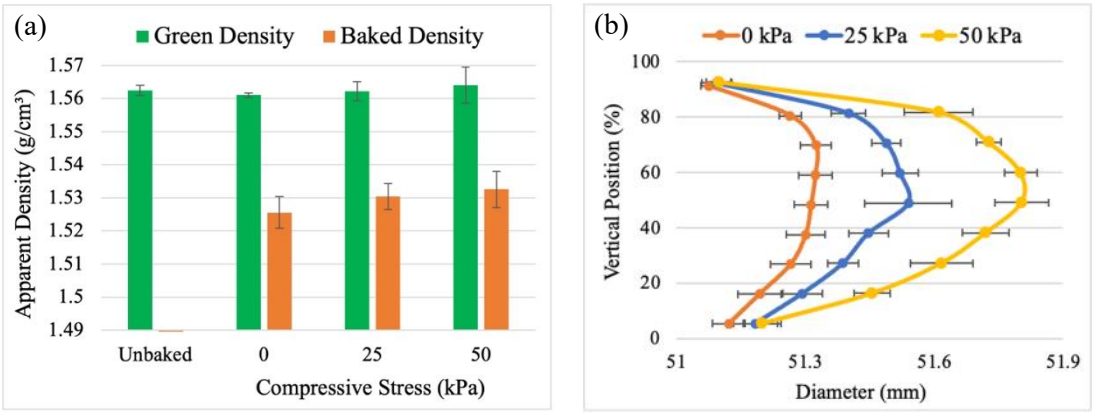

Figure 7. (a): Green and baked apparent densities of all anodes, (b): Barreling effect in the anodes baked with compressive stresses. Error bars show the standard deviations.

Figure 7-b shows the diameter variation as a function of the vertical position on the anode surface, normalized based on the average length of each sample. The scale for diameter is chosen in a narrow range to better visualize the variations. As depicted in this graph, the barreling effect is evident for all samples, but it is more pronounced in the anodes baked under higher stress. It is also interesting to notice the barreling effect in the sample baked with no compressive stress. This may suggest that the barreling effect also represents the sample swelling, which is due to the generation of volatiles and buildup of the internal pressure. In the middle part, the internal pressure should be higher than that on top and bottom since the volatiles can also escape from the extremities.

The much more pronounced barreling effect under stress suggests that the compressive stress has significant contribution to this phenomenon. In fact, the internal pressure, due to pitch devolatilization, resulted in approximately 0.5 % of the diameter change under 0 kPa, while anode diameter was increased notably by 1.4 % during baking under 50 kPa stress.

- **Specific Electrical Resistivity**

Figure 8 represents the specific electrical resistivity (SER) of the baked anodes determined using standard and Van der Pauw (VDP) methods. The SER, assessed by the standard method, decreases

by increasing the compressive stress, which is in accordance with Barry's results [9, 16]. The difference of the mean SER was also indicated to be statistically significant using one-way ANOVA (*p*-value was calculated 3.421×10^{-5}). Anode deformation due to the high stresses reduces the contact distance between the coke aggregates allowing the electrical current to pass more easily through the anode, resulting in a lower SER.

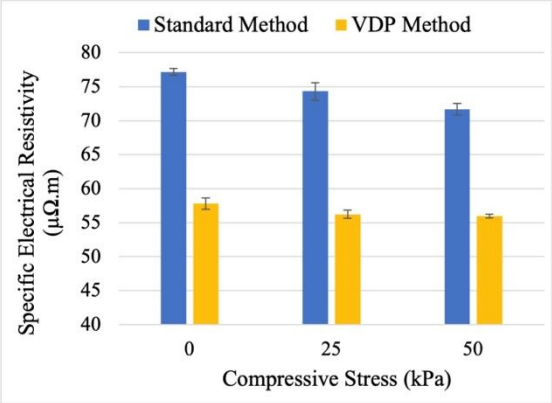

Figure 8. Electrical resistivity of baked anodes. Error bars show the standard deviations.

The SER determined by the VDP method (Figure 8) is not only significantly less than that of the standard method, but its variation is also relatively smaller. The maximum SER difference for the standard method is 7.7 % between 0 kPa and 50 kPa. This difference obtained using VDP method is 3.2 %, even though it is still statistically significant based on one-way ANOVA (*p*-value was calculated 0.023). In fact, VDP method is conducted on small-scale samples, and hence, the effect of the structural imperfections, such as microcracks and coarse particles possessing their own flaws, can be reduced to some extent [1, 14].

- **Pitch Tracer**

Figures 9 (a–d) demonstrate XRF mapping results of bismuth (BiLα) on both green sample (Figure 9-a) and baked samples (Figure 9-b, c, d) with different compressive stresses exerted during baking. It needs to be noted that the XRF mappings that are shown were obtained from one sample only, but they are representative of the three images resulting from each sample and condition. Python programming was used for image analysis to extract the pixel intensity as a function of the position in the cross-section of the specimen. For every XRF image, the Bi intensities were averaged in 40 distinct radii having a constant width of 0.643 mm. The distribution of Bi intensities along the radii were plotted as a function of distance from the center for three samples at each condition. Figures 9 (e–h) depict the average of three curves with the standard deviation of the averages. It is also worth mentioning that the smallest circular band is composed of 55348 pixels.

Bi is homogeneously distributed over the green specimen (Figure 9-e), implying that the stress exerted during forming did not impact the pitch distribution. In all baked anodes, on the other hand, the Bi concentration increases gradually from the center up to a radius around 21 mm (Figure 9-f, g, h). Since Bi was only contained in the pitch, this indicates a movement of the pitch toward the surface of the anode during baking. Nevertheless, at radii larger than 21 mm, the Bi intensity decreases sharply in all baked samples and regardless of the applied stress. Therefore, only a small trace of Bi content is observed on the edge of the baked specimens.

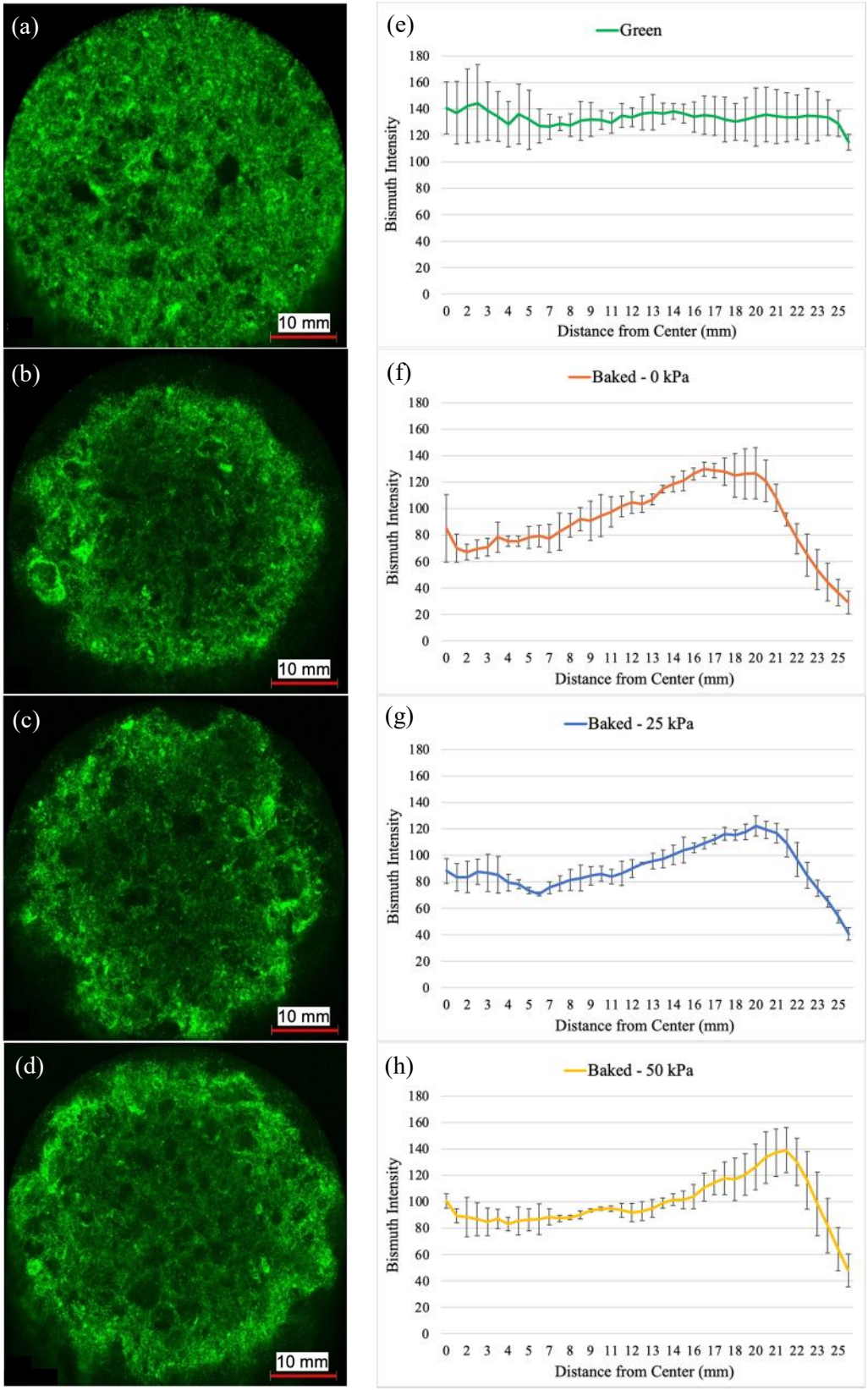

Figure 9. (a–d): Elemental mapping of Bi in the cross-section of the anodes (XRF mapping, Bi-Lα), (e–h): Bi intensity in different distances from the center of the sample. Error bars indicate the standard deviations.

The average concentration of bismuth in three positions of the cross-section of all specimens was obtained using XRF analysis, as illustrated in Figure 10. The percentage of Bi in the green anodes is near 0.13 %, which is close to the theoretical value of 0.15 %, considering the Bi/pitch and pitch/anode ratios, with no significant variation in all areas, similar to that observed in the elemental mapping (Figure 9-a). In each position, the Bi concentration decreases by at least 50 % after baking. On the other hand, the Bi concentration in all baked samples increases by approximately 60 % from position 1 (center) to position 3 (edge). No significant difference is observed in the average concentration of Bi for various compressive stresses, confirming the XRF mapping results (Figure 9).

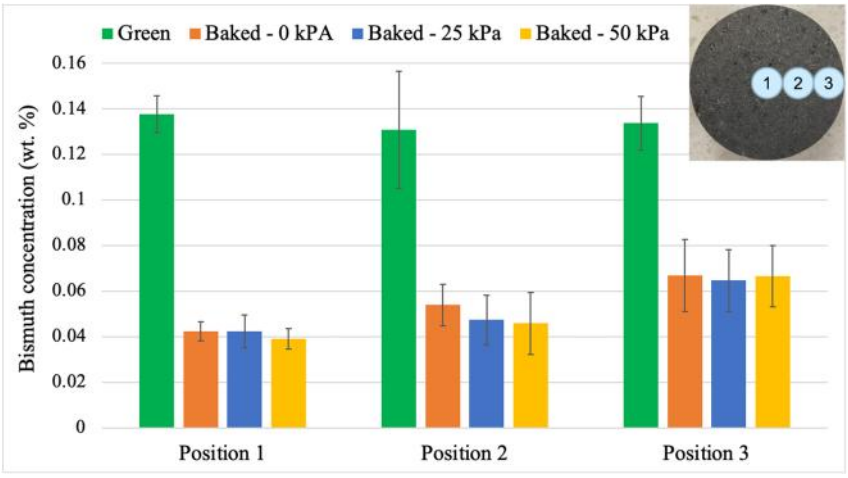

Figure 10. XRF elemental composition of green and baked anodes in three positions. Error bars indicate the standard deviations.

From the chemical point of view, bismuth oxide can be reduced by carbon at a temperature above its melting point (850 °C), according to the Equation (5), and Equation (6) [17].

$$Bi_2O_{3\,(l)} + 3C_{\,(s)} = 2Bi_{\,(l)} + 3CO_{\,(g)} \qquad \Delta G_{927} = -404.7\ kJ \qquad (5)$$

$$Bi_2O_{3\,(l)} + 1.5C_{\,(s)} = 2Bi_{\,(l)} + 1.5CO_{2\,(g)} \qquad \Delta G_{927} = -345.8\ kJ \qquad (6)$$

At 927 °C, the Gibbs free energy (ΔG) is calculated using FactSage thermochemical software [18]. It signifies that these reactions occur spontaneously during the baking process. Given that the maximum baking temperature was 1100 °C with 20 h soaking time, the reduced bismuth would be in liquid form and very likely to evaporate since its vapor pressure at this temperature (1500 Pa) is greater than the ambient pressure [19]. As a result, Bi can easily evaporate from the sample surface, leaving behind a Bi-depleted layer. These data explain the Bi-mapping results presented in Figure 9 and the significant decrease of Bi concentration after baking.

Figure 11-a represents a Backscattered Electron (BSE) image obtained from the polished surface of the sample baked under σ_3 = 50 kPa. The bright spots in the BSE indicate the presence of a high-atomic number element, verified to be Bi by using EDS spectra of "Spot 2" (Figure 11-b). Nevertheless, the atomic percentages indicate the Bi/O ratio is more than twice, which is entirely different from the expected proportion of 2/3 in Bi_2O_3 shown in Figure 6-d. Therefore, it confirms that the chemical bond of some Bi_2O_3 content was broken during the baking process and was subsequently reduced to liquid Bi at a temperature above its melting point (850 °C) [17].

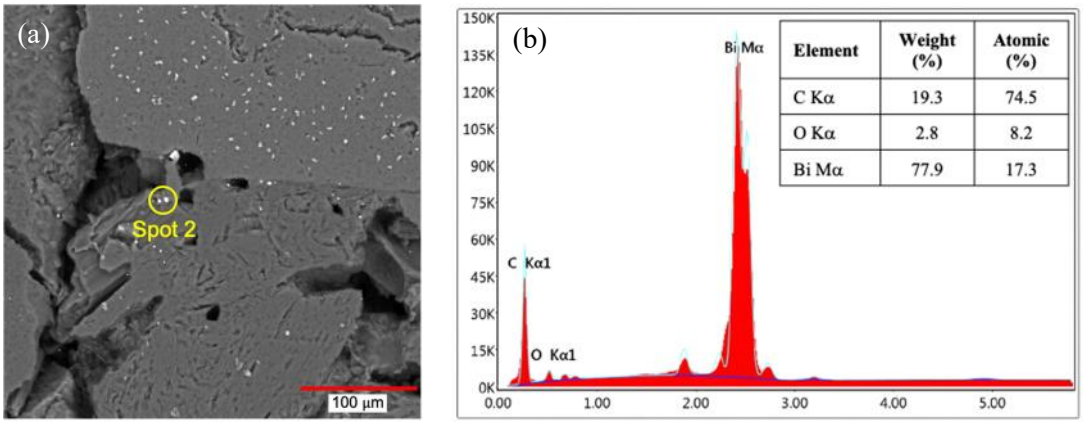

Figure 11. (a): BSE image of the baked anode, (b): EDS spectra of Spot 2.

Overall, the results confirm that pitch tends to move toward the anode surface during baking. They also suggest that this pitch movement is primarily caused by the internal pressure due to the volatile generation, since pitch squeezing was also detected within no-stress baking. Furthermore, pitch tracer evaluation showed to be a helpful methodology which is used to study the correlation of pitch squeezing with anode sticking in future work. However, the impact of higher mechanical stress on pitch distribution could not be demonstrated using this pitch marker due to the Bi evaporation. For further experiments, it is intended to develop an alternative stable pitch marker in order to affirm the evolution of pitch squeezing by mechanical stress as well as its correlation with anode sticking.

4. Conclusions

The objective of this work was to determine if anode stacking in industrial furnaces can influence pitch squeezing out of the anodes during baking, which may contribute to the anode sticking. Bismuth oxide was selected as a marker to measure the distribution of pitch in lab-scale anodes made with optimum pitch ratio. The anodes were subsequently baked under uniaxial compressive stresses corresponding to the position of each industrial anode ($\sigma_1 = 0$ kPa, $\sigma_2 = 25$ kPa, $\sigma_3 = 50$ kPa). Anode characterization demonstrated that by raising the stresses, the specific electrical resistivity decreased, while the increase of baked apparent density was not statistically significant. XRF analysis determined a uniform distribution of Bi in green anodes, while higher Bi concentration was detected in the vicinity of the edge of the anode. It indicated that the pitch was moving toward the anode surfaces during the baking process. Nevertheless, the influence of different mechanical stresses on pitch squeezing could not be established since the Bi element evaporated during baking. SEM and EDS analyses also verified the reduction of Bi_2O_3 to Bi after the baking process. As a consequence, pitch marker development showed to be a beneficial method to trace pitch distribution and ultimately, correlate that with anode sticking phenomenon. However, this development needs to be pursued regarding tracer material to prove the hypothesis of the effect of mechanical stress on pitch squeezing. Further efforts are required to develop an alternative stable marker to reveal pitch squeezing due to the compressive stress and its relationship with anode sticking.

5. Acknowledgment

The authors would like to thank Alcoa Corporation (Alcoa), the Natural Science and Engineering Research Council of Canada (NSERC), Université Laval, and the Aluminium Research Centre (REGAL) for their financial support. The technical support of Mr. Nelson Landry and Mr. Hugues Ferland is greatly appreciated.

6. References

1. Asem Hussein, Donald Picard, and Houshang Alamdari, Biopitch as a binder for carbon anodes: impact on carbon anode properties, *ACS Sustainable Chemistry & Engineering,* vol. 9, no. 12, 4681-4687, 2021, https://doi.org/10.1021/acssuschemeng.1c00618 .
2. Gøril Jahrsengene, Coke Impurity Characterisation and Electrochemical Performance of Carbon Anodes for Aluminium Production, PhD diss., Norwegian University of Science and Technology (NTNU), 2019.
3. Arne Petter Ratvik, Roozbeh Mollaabbasi, and Houshang Alamdari, Aluminium production process: from Hall–Héroult to modern smelters, *ChemTexts,* vol. 8, no. 2, 10, 2022, https://doi.org/10.1007/s40828-022-00162-5 .
4. D Kocaefe et al., A kinetic study of pyrolysis in pitch impregnated electrodes, *The Canadian Journal of Chemical Engineering,* vol. 68, no. 6, 988-996, 1990, https://doi.org10.1002/cjce.5450680614 .
5. Kirstine Louise Hulse, *Raw materials, formulation and processing parameters* (R&D Carbon Ltd., Switzerland). R & D Carbon Limited, 2000.
6. Adéline Paris et al., Development of a soft sensor for detecting overpitched green anodes, *Light Metals 2020,* 1176-1182, 2020, https://doi.org/10.1007/s11663-021-02335-y .
7. Kevin Williams, "The readiness and compatibility of a modern anode handling and cleaning system for industry 4.0 technologies," in *Light Metals 2021*: Springer, 2021, pp. 957-964, https://doi.org/10.1007/978-3-030-65396-5_126 .
8. Bienvenu Ndjom et al., Challenges and Opportunities of Vacuum Compaction: Lessons Learnt from Retrofitting EGA-JA Paste Plant to Vacuum Compaction, *Light Metals 2019,* 1213-1220, 2019.
9. Thierno Saidou Barry et al., "Investigation of the Stacking Effects on the Electrical Resistivity of Industrial Baked Anodes," presented at the Light Metals 2023, 2023.
10. Asem Hussein, Bio-pitch as a potential binder in carbon anodes for aluminum production, PhD diss., Université Laval, 2021.
11. Julien Lauzon-Gauthier, Carl Duchesne, and Jayson Tessier, A machine vision sensor for quality control of green anode paste material, *JOM,* vol. 72, 287-295, 2020.
12. Kamran Azari Dorcheh, Investigation of the materials and paste relationships to improve forming process and anode quality, PhD diss., Université Laval, 2013.
13. Amrita Priyadarshini, CP Kiran, and K Suresh, Effect of Friction on Barreling during cold Upset Forging of Aluminium 6082 Alloy Solid cylinders, in *IOP Conference Series: Materials Science and Engineering*, 2018, vol. 330, no. 1: IOP Publishing, p. 012072, https://doi.org/10.1088/1757-899X/330/1/012072 .
14. Geoffroy Rouget et al., Electrical Resistivity Measurement of Carbon Anodes Using the Van der Pauw Method, *Metals,* vol. 7, no. 9, 369, 2017, https://doi.org10.3390/met7090369.
15. Ilio Miccoli et al., The 100th anniversary of the four-point probe technique: the role of probe geometries in isotropic and anisotropic systems, *Journal of Physics: Condensed Matter,* vol. 27, no. 22, 223201, 2015.
16. Thierno Saidou Barry, Effet de l'empilement des anodes de carbone pendant la cuisson sur leur densification et sur leur résistivité électrique, MSc diss., Université Laval, 2020.
17. MM Sarafraz et al., Experimental investigation of the reduction of liquid bismuth oxide with graphite, *Fuel Processing Technology,* vol. 188, 110-117, 2019, https://doi.org/10.1016/j.fuproc.2019.02.015 .
18. Christopher W Bale et al., Reprint of: FactSage thermochemical software and databases, 2010–2016, *Calphad,* vol. 55, 1-19, 2016, https://doi.org/10.1016/j.calphad.2016.07.004 .
19. Dean Massey, Lyon King, and Jason Makela, Development of a direct evaporation bismuth Hall thruster, in *44th AIAA/ASME/SAE/ASEE Joint Propulsion Conference & Exhibit*, 2008, p. 4520.